KIAA1429-mediated ZFPM2-AS1 m^{6}A modification promotes the proliferation, migration and invasion of osteosarcoma cells

YUANZHUANG ZHANG[1*], YUXIN BAO[1*], HANJIE ZHAI[1], CHENGHAO LI[1], HONGCHAO SHI[1], KEYANG GONG[2] and XIAOHE BAO[1]

[1]Fourth Department of Orthopedic Surgery, Central Hospital Affiliated to Shenyang Medical College, Shenyang, Liaoning 110024, P.R. China; [2]School of Basic Medicine, Shenyang Medical College, Shenyang, Liaoning 110000, P.R. China

Received September 24, 2024; Accepted May 16, 2025

DOI: 10.3892/ol.2025.15199

Abstract. Osteosarcoma is the most prevalent malignant bone tumor in pediatric and adolescent populations. N^6-methyladenosine (m^{6}A) is a post-transcriptional modification of RNA, and the most prevalent internal chemical modification of mRNA. KIAA1429, also known as virus-like m^{6}A methyltransferase-associated, is a key component of the m^{6}A methyltransferase complex, and the largest protein within this complex. Long non-coding RNAs (lncRNAs) are a class of transcripts >200 nucleotides in length that are able to regulate gene expression. Friend of GATA family member 2-antisense 1 (ZFPM2-AS1) is a lncRNA that has been observed to exhibit aberrantly elevated expression in gastric cancer. The present study aimed to explore the expression levels of KIAA1429 and ZFPM2-AS1 in osteosarcoma tissues and 143B and MG63 osteosarcoma cell lines. The results of bioinformatics analysis, reverse transcription-quantitative PCR (qPCR) and western blotting revealed that the expression of KIAA1429 and ZFPM2-AS1 in osteosarcoma tissues and cell lines was upregulated compared with that in the corresponding normal tissues or cells. The association between KIAA1429-mediated m^{6}A modifications and ZFPM2-AS1 stability in osteosarcoma cells was confirmed using m^{6}A-methylated RNA immunoprecipitation-qPCR and actinomycin D assays. In addition, in Cell Counting Kit-8 and Transwell assays KIAA1429 overexpression promoted the proliferation, invasion and migration of 143B and MG63 osteosarcoma cells, and these promotive effects were attenuated by ZFPM2-AS1 knockdown. These findings suggest a potential novel approach for molecular therapy in the treatment of osteosarcoma.

Correspondence to: Professor Xiaohe Bao, Fourth Department of Orthopedic Surgery, Central Hospital Affiliated to Shenyang Medical College, 5 South Seven West Road, Tiexi, Shenyang, Liaoning 110024, P.R. China
E-mail: 114343110@qq.com

*Contributed equally

Key words: osteosarcoma, KIAA1429, ZFPM2-AS1, m^{6}A, molecular mechanisms

Introduction

Osteosarcoma is the most prevalent malignant bone tumor in children and adolescents, with an estimated annual incidence of 3-5 cases per million individuals under 20 years of age globally. It originates from primitive bone mesenchymal cells, typically manifests in the metaphysis of long bones, and exhibits rapid growth and progression (1). Advances in treatment techniques for osteosarcoma, including surgery combined with neoadjuvant radiotherapy and chemotherapy, have led to a significant improvement in the 5-year overall survival rate of patients with osteosarcoma (2). However, recurrent metastasis remains a persistent challenge, and the molecular mechanisms underlying osteosarcoma remain poorly understood (3). Consequently, it is urgently necessary to elucidate the molecular mechanisms underlying the progression of osteosarcoma and identify novel therapeutic targets.

N^6-methyladenosine (m^{6}A) is the most prevalent internal chemical modification of mRNA (4) and a key post-transcriptional modification of RNA. The effects of this modification on the regulation of RNA depend on dynamic interactions between methyltransferases, demethylation enzymes and binding proteins, which are also known as writers, erasers and readers, respectively (5). Recently, m^{6}A-associated enzymes have been reported to perform roles in several types of tumor, including hepatocellular carcinoma (6), gastric cancer (7), lung cancer (8), glioma (9) and osteosarcoma (10). KIAA1429, also known as virus-like m^{6}A methyltransferase associated, is a component of the intact m^{6}A methyltransferase complex, and the largest protein within this complex (11). KIAA1429 facilitates m^{6}A methylation by recruiting the core components methyltransferase-like 3 (METTL3), METTL14 and Wilms tumor 1-associated protein (WTAP) to specific regions of target RNA. KIAA1429 has also been reported to play a role in several types of tumor (12). KIAA1429 mediates the m^{6}A modification of carbohydrate sulfotransferase 11 (CHST11) mRNA, leading to the recruitment of YTH domain-containing family (YTHDF) protein 2 (YTHDF2), which reduces the stability and expression of CHST11, thereby promoting the proliferation of diffuse large B-cell lymphoma cells (13).

Additionally, KIAA1429 is highly expressed in hepatocellular carcinoma, where it facilitates tumor proliferation by reducing the stability of Rho family GTPase 3. In osteosarcoma, KIAA1429 has been identified as a key factor that promotes the proliferation, migration and invasion of osteosarcoma cells through the KIAA1429/JAK2/STAT3 signaling pathway (14). However, the precise role of KIAA1429 in osteosarcoma has yet to be fully elucidated; therefore, further comprehensive evaluation of KIAA1429 is necessary.

Long non-coding RNAs (lncRNAs) are a class of transcripts that are >200 nucleotides in length (15). Due to the absence of open reading frames, they do not encode polypeptides or proteins (16). However, there is a substantial body of evidence showing that lncRNAs have a pivotal role in the regulation of gene expression. Aberrant RNA expression has been shown to regulate gene expression by either silencing or activation (17). m^6A modifications can regulate the function of lncRNAs by altering their structure, thereby inducing the binding of RNA-binding proteins. Furthermore, m^6A modifications can influence the triple-helical structure of lncRNAs, which may affect their ability to interact with DNA (18,19). KIAA1429 has been demonstrated to upregulate the expression of LINC01106 via m^6A modification, thereby facilitating the proliferation of lung adenocarcinoma cells (20). Friend of GATA family member 2-antisense 1 (ZFPM2-AS1) is a lncRNA transcribed from the antisense strand of the ZFPM2 gene, which encodes a zinc finger protein. It was initially identified to be aberrantly overexpressed in gastric cancer.

Additionally, ZFPM2-AS1 has been reported to play a role in a variety of other tumor types, including lung (21), esophageal (22) and thyroid (23) cancer. However, the function of ZFPM2-AS1 in osteosarcoma, and the potential for m^6A modification of ZFPM2-AS1, have yet to be elucidated. Therefore, the present study aimed to resolve these issues.

The present study evaluated the expression of KIAA1429 and ZFPM2-AS1 in osteosarcoma. In addition, the effect of KIAA1429 knockdown on the proliferation, migration and invasion of 143B and MG63 osteosarcoma cell lines was examined. Furthermore, the impact of KIAA1429 overexpression on the m^6A modification level and stability of ZFPM2-AS1 was investigated. Finally, the ability of ZFPM2-AS1 knockdown to attenuate KIAA1429-mediated pro-proliferative, migratory and invasive effects in osteosarcoma cells was assessed.

Materials and methods

Bioinformatics analysis and software availability. The expression levels of KIAA1429 and ZFPM2-AS1 in sarcomas and normal tissue were analyzed using data from The Cancer Genome Atlas (TCGA) via the UALCAN tool (https://ualcan.path.uab.edu/index.html) (24). The association between the expression of ZFPM2-AS1 in sarcoma tissues and the overall survival of patients was analyzed using TCGA data via the Gene Expression Profiling Interactive Analysis 2 (GEPIA2) database (http://gepia2.cancer-pku.cn/#index) (25). The expression of KIAA1429 in 18 pairs of osteosarcoma and non-tumoral tissues was analyzed using the GSE99671 osteosarcoma-related dataset from the Gene Expression Omnibus (GEO) database (https://www.ncbi.nlm.nih.gov/geo/info/geo2r.html). The correlation between the expression of KIAA1429 and other genes in 87 osteosarcoma tissue samples from TCGA-TARGET-osteosarcoma (OS) database was analyzed using PDX for Childhood Cancer Therapeutics online analysis software. The 20 genes identified as having the highest expression correlation were subsequently downloaded and collated. The correlation between the expression of KIAA1429 (probe ID: 25962) and ZFPM2-AS1 (probe ID: 102723356) was analyzed in 52 samples from the GEO osteosarcoma-related dataset GSE87624. Sarcoma data were also downloaded from TCGA database to analyze the correlation between KIAA1429 and ZFPM2-AS1 expression in 260 sarcoma tissue samples. The gene sequence of ZFPM2-AS1 (NR_125796.1) was retrieved from the National Center for Biotechnology Information (NCBI) database (https://www.ncbi.nlm.nih.gov/gene/?term=ZFPM2-AS1). Finally, m^6A modification sites in the ZFPM2-AS1 sequence were predicted using SRAMP (http://www.cuilab.cn/sramp/) online bioinformatics software (26).

Patients and tissue samples. A total of 20 pairs of surgically resected osteosarcoma and paraneoplastic tissue samples were collected from the Central Hospital Affiliated to Shenyang Medical College (Shenyang, China) and Liaoning Provincial Cancer Hospital (Shenyang, China). The samples were collected from 8 male and 12 female patients (median age, 16 years; age range, 8-22 years) who underwent surgery between April 2016 and April 2022. All patients were clinically and pathologically diagnosed with osteosarcoma. Written informed consent was obtained from all adult participants and from the parents or legal guardians of participants <18 years of age. The study protocol was approved by the Medical Ethics Committee of the Central Hospital Affiliated to Shenyang Medical College (approval no. 2022DEC12-7).

Cell culture. The hFOB1.19 human osteoblast cell line and the 143B and MG63 osteosarcoma cell lines were obtained from The Cell Bank of Type Culture Collection of The Chinese Academy of Sciences. Characterization of the three cell lines using short tandem repeat analysis demonstrated that these cells were not cross-contaminated. The hFOB1.19 osteoblasts were cultured in Gibco® DMEM/F12 medium, the MG63 cells were cultured in Minimal Essential Medium, and the 143B cells were cultured in RPMI-1640 medium (all from Thermo Fisher Scientific, Inc.). The media were supplemented with 10% (v/v) Gibco fetal bovine serum (Gibco; Thermo Fisher Scientific, Inc.) and a solution of penicillin and streptomycin (penicillin, 100 U/ml; streptomycin, 0.1 mg/ml). All three cell lines were cultured in a cell culture incubator in an atmosphere containing 5% CO_2. The hFOB1.19 cells were maintained at 34˚C, while the 143B and MG63 cells were cultured at 37˚C.

RNA extraction and reverse transcription-quantitative PCR (RT-qPCR). Total RNA was extracted from cells and tissues using an Invitrogen TRIzol® Plus RNA Purification Kit (Thermo Fisher Scientific, Inc.) following the manufacturer's instructions. Reverse transcription was performed with the PrimeScript RT Master Mix (Takara Bio, Inc., cat. no. RR036A) in a 20 μl reaction containing 1 μg total RNA, 5X RT Master Mix, and RNase-free water. The thermal protocol included 37˚C for 15 min, 85˚C for 5 sec, and a final

hold at 4˚C. qPCR was carried out using the TB Green Premix Ex Taq II kit (cat. no. RR820A; Takara Bio, Inc.) under the following conditions: Initial denaturation at 95˚C for 30 sec, followed by 40 cycles of 95˚C for 5 sec and 60˚C for 30 sec. GAPDH served as the internal reference gene, and relative gene expression was calculated using the $2^{-\Delta\Delta Cq}$ method. All primers were synthesized by Takara Bio, Inc., and sequences are listed in Table SI.

Western blot analysis. Proteins were extracted from cells and tissues using a protein extraction kit (cat. no. GM1001; Wuhan Servicebio Technology Co., Ltd.). Protein concentrations were determined using a BCA protein assay kit (Wuhan Servicebio Technology Co., Ltd.). A total of 25 μg protein per lane was denatured in a water bath at 100˚C for 5 min, followed by separation using 8% sodium dodecyl sulfate-polyacrylamide gel electrophoresis (SDS-PAGE; cat. no. G2176; Wuhan Servicebio Technology Co., Ltd.) at a constant voltage of 120 V. Proteins were transferred to polyvinylidene fluoride (PVDF) membranes (cat. no. G6044-0.45; Wuhan Servicebio Technology Co., Ltd.) at a constant current of 400 mA. Membranes were blocked with NcmBlot Rapid Blocking Buffer (cat. no. P30500; NCM Biotech) at room temperature (25˚C) for 15 min. Primary antibodies against KIAA1429 (cat. no. ab271136; Abcam; 1:1,000 dilution) and GAPDH (cat. no. ab9485; Abcam; 1:2,500 dilution) were incubated with the membranes at 4˚C overnight. After washing with Tris-buffered saline containing 0.1% Tween 20 (TBST), membranes were incubated with horseradish peroxidase (HRP)-conjugated goat anti-rabbit IgG secondary antibody (cat. no. ab205718; Abcam; 1:10,000 dilution) at room temperature for 1 h. Protein bands were visualized using an ultra-sensitive ECL chemiluminescence detection kit (cat. no. G2074; Wuhan Servicebio Technology Co., Ltd.) and imaged with a gel documentation system (ChemiScope 6100; Shanghai Qinxiang Scientific Instrument Co., Ltd.). Protein expression levels were quantified using ImageJ software (Version 1.53; National Institutes of Health) and normalized to GAPDH.

Cell transfection. Two short hairpin RNAs (shRNAs) targeting the KIAA1429-specific junction region (shKIAA1429-1 and shKIAA1429-2), their corresponding negative control shRNAs (shNCs), a KIAA1429 overexpression plasmid (oeKIAA1429), and the empty plasmid vector pCMV6-Entry were designed and synthesized by Hanheng Biotechnology (Shanghai) Co., Ltd. shRNAs (final concentration: 50 nM) and plasmids (final concentration: 2 μg/ml) were transfected into 143B, MG63, and hFOB1.9 cells using the Invitrogen Lipofectamine® 3000 reagent (cat. no. L3000001; Thermo Fisher Scientific, Inc.) under standard conditions (37˚C for 6 h), followed by replacement with complete culture medium. Additionally, a small interfering RNA (siRNA) targeting ZFPM2-AS1 (siZFPM2-AS1) and its negative control siRNA (siNC) were designed by Guangzhou RiboBio Co., Ltd. and transiently transfected into osteosarcoma cells at a final concentration of 50 nM using the RiboFect® CP Transfection Kit (cat. no. C10511-05; Guangzhou RiboBio Co., Ltd.), according to the manufacturer's protocol. Cells were harvested 48 h post-transfection for subsequent experiments. The sequences of shRNAs, siRNAs, and oeKIAA1429 are listed in Table SI.

Cell Counting Kit-8 (CCK-8) assay. 143B and MG63 cells were inoculated into 96-well plates at a density of $2x10^3$ cells/well, and cultured in a cell culture incubator at 37˚C in an atmosphere containing 5% CO_2. At 24, 48, 72 and 96 h, 10 μl CCK-8 solution (cat. no. G4103; Wuhan Servicebio Technology Co., Ltd.) was added to each well for 2 h. Following this, the 96-well plates were removed from the incubator and the absorbance at 450 nm was measured using a microplate reader (Multiskan FC Photometer; Thermo Fisher Scientific, Inc.).

Transwell assay. Different densities of the 143B and MG63 cells were used, according to whether the Transwell assay was used to assess migration ($4x10^4$ cells) or invasion ($8x10^4$ cells). The cells were cultured in the upper chamber of the Transwell apparatus (Corning, Inc.). After 24 h at 37˚C, the cells in the upper chamber were scraped off and those on the lower side of the Transwell membrane were fixed with anhydrous ethanol prior to staining with 0.1% crystal violet staining solution (cat. no. G1014; Wuhan Servicebio Technology Co., Ltd.) for 30 min at room temperature. Following a rinse with running water, the migrated or invaded cells were observed under an inverted microscope (Olympus Corporation). For invasion assays, the upper chambers of Transwell inserts (Corning, Inc.) were pre-coated with Matrigel Basement Membrane Matrix (Corning, cat. no. 354234) diluted 1:8 in serum-free medium, followed by polymerization at 37˚C for 1 h. Cell densities were adjusted according to assay type: $4x10^4$ cells/well for migration and $8x10^4$ cells/well for invasion. Cells were suspended in serum-free RPMI-1640 medium (for 143B) or MEM (for MG63) and added to the upper chamber. The lower chamber contained complete medium with 10% fetal bovine serum (Thermo Fisher Scientific, Inc.) as a chemoattractant. After 24 h incubation at 37˚C in 5% CO_2, non-invaded cells on the upper membrane surface were removed using a cotton swab. Cells on the lower side were fixed with anhydrous ethanol for 15 min, stained with 0.1% crystal violet (Wuhan Servicebio, cat. no. G1014) for 30 min, and rinsed with PBS. Images were captured using an inverted microscope (Olympus Corporation) at 200x magnification. Cell counts were quantified from five random fields per membrane.

m^6A-methylated RNA immunoprecipitation-qPCR (MeRIP-qPCR) assay. The assay was conducted using an m^6A-Methylated RNA Immunoprecipitation Kit (cat. no. 11096.6; Guangzhou Ribobio Co., Ltd.) in accordance with the manufacturer's instructions. In brief, the collected RNA was fragmented using RNA Fragmentation Buffer. A fraction (one-tenth) of the fragmented RNA was retained as an input control group for subsequent analysis, while the remainder was used for m^6A immunoprecipitation (IP). Anti-m^6A magnetic beads were prepared using m^6A antibody (cat. no. ab151230; dilution, 1:500). The fragmented RNA was added to the MeRIP reaction mixture, and incubated with anti-m^6A magnetic beads. After incubation, the mixture was centrifuged at 1,000 x g for 3 min at 4˚C and the supernatant was discarded. The magnetic beads were then washed, followed by elution of the bound RNA. The eluted RNA fragments were recovered and purified using the GeneJET RNA Purification Kit (cat. no. K0731; Thermo Fisher Scientific, Inc.). The

recovered RNA was designated as the IP group. Subsequently, the input and IP groups were analyzed by RT-qPCR.

Actinomycin D assay. The collected cells ($2x10^6$ cells) were transferred to 6-well plates and cultured to a confluency of 80%. The cells were then treated with 2 μg/ml actinomycin D reagent (cat. no. 50-76-0; MedChemExpress). Total cellular RNA was extracted at 0, 4, 8 and 12 h and analyzed by RT-qPCR.

Statistical analysis. Statistical analyses were performed using GraphPad Prism 8.0 software (Dotmatics). Results are expressed as the mean ± standard deviation. For comparative analyses involving two groups, paired tests were used to evaluate results from paired patient tissue samples: a paired t-test was applied for normally distributed data, whereas the Wilcoxon signed-rank test was applied for non-normally distributed data. Unpaired t-tests were used for the comparison of two independent samples with normally distributed means. In datasets comprising three or more groups, one-way analysis of variance followed by Tukey's post hoc test was used for normally distributed data, and Kruskal-Wallis test was performed followed by Dunn's post hoc analysis for non-normally distributed data. Linear correlation analyses were performed, with Pearson correlation coefficients calculated for normally distributed data and Spearman correlation coefficients for non-normally distributed data. Each experiment was replicated thrice. $P<0.05$ was considered to indicate a statistically significant difference.

Results

KIAA1429 is upregulated in osteosarcoma tissues and cell lines. Bioinformatics analysis was performed to investigate the expression of KIAA1429 in osteosarcoma and normal tissues. Analysis of TCGA data revealed that the expression of KIAA1429 in sarcoma was markedly elevated compared with that in normal tissues. The expression of KIAA1429 was also analyzed in the GSE99671 dataset from the GEO database, which revealed that the expression of KIAA1429 in sarcoma tissues was significantly higher compared with that in the corresponding normal tissues (Fig. 1A and B). Subsequently, 20 pairs of osteosarcoma and paraneoplastic tissues collected from patients were examined by RT-qPCR analysis, which revealed a significant upregulation of KIAA1429 expression in the osteosarcoma tissues (Fig. 1C). In addition, the western blot analysis of five pairs of osteosarcoma and paraneoplastic tissues confirmed that expression of KIAA1429 protein was significantly upregulated in the osteosarcoma tissues (Fig. 1D). Subsequently, normal osteoblast and osteosarcoma cell lines were analyzed using RT-qPCR and western blotting. The results demonstrated that KIAA1429 mRNA and protein expression levels in the 143B and MG63 osteosarcoma cells were significantly higher compared with those in the hFOB1.19 cells (Fig. 1E and F). The findings of the bioinformatics analysis, tissue and cellular experiments collectively demonstrate that KIAA1429 expression is upregulated in osteosarcoma.

KIAA1429 knockdown inhibits the proliferation, migration and invasion of osteosarcoma cells. The impact of KIAA1429 on osteosarcoma cell proliferation, migration and invasion was investigated in functional assays of 143B and MG63 cells transfected with shKIAA1429-1, shKIAA1429-2 and shNC. The successful establishment of KIAA1429 knockdown was verified in the two cell lines via RT-qPCR and western blotting (Fig. 2A-D). A CCK-8 cell proliferation assay was then performed to assess the impact of KIAA1429 knockdown on cell proliferation. The results demonstrated that KIAA1429 knockdown significantly inhibited the proliferative capability of the 143B and MG63 cells compared with that of the corresponding shNC controls (Fig. 2E and F). Subsequently, Transwell assays were performed to evaluate the migration and invasion of the 143B and MG63 cells. The results revealed that the migratory and the invasive capabilities of the cells were significantly diminished following the knockdown of KIAA1429 (Fig. 2G and H). Together, these findings suggest that KIAA1429 promotes the proliferation, migration and invasion of 143B and MG63 osteosarcoma cells.

KIAA1429-mediated m^6A modification is associated with ZFPM2-AS1 stability in osteosarcoma cells. Expression data from 87 osteosarcoma tissues in TCGA-TARGET-OS database were analyzed to identify genes whose expression levels significantly correlated with KIAA1429 expression levels. Of the top 20 genes whose expression correlated with that of KIAA1429, ZFPM2-AS1 was the only lncRNA identified (Table SII and Fig. 3A). The online tool SRAMP was then used to predict the presence of theoretical m^6A modification sites (RRACH sequences) in the ZFPM2-AS1 sequence, and six such sites were identified (Fig. S1A). Based on this finding, the potential regulation of ZFPM2-AS1 by KIAA1429 was investigated. ZFPM2-AS1 expression levels were found to correlate with KIAA1429 expression levels in the GSE87624 osteosarcoma-related dataset as well as in sarcoma tissues in TCGA database (Fig. 3B and C). Similarly, reduced expression levels of ZFPM2-AS1 were observed following KIAA1429 knockdown in 143B and MG63 cells (Fig. 3D and E). hFOB1.19 cells overexpressing KIAA1429 were successfully constructed, as confirmed by western blotting (Fig. S1B). RT-qPCR results revealed a corresponding increase in the expression level of ZFPM2-AS1, further supporting a positive association between KIAA1429 and ZFPM2-AS1 expression (Fig. S1C). Although ZFPM2-AS1 has been characterized as an oncogene in numerous types of tumor, its specific role in osteosarcoma remains unclear. Analysis of data from TCGA revealed that ZFPM2-AS1 expression is upregulated in sarcoma tissue compared with normal tissue, and high ZFPM2-AS1 expression is associated with a poorer overall survival profile in patients with sarcoma (Fig. 3F and G). Subsequently, the expression levels of ZFPM2-AS1 were assessed in 20 pairs of osteosarcoma and paraneoplastic tissues via RT-qPCR analysis. The results demonstrated that the expression of ZFPM2-AS1 in osteosarcoma tissues was upregulated compared with that in paraneoplastic tissues (Fig. 3H). Furthermore, analysis of the expression of ZFPM2-AS1 in hFOB1.19, 143B and MG63 cells. revealed that ZFPM2-AS1 expression in the osteosarcoma cell lines was elevated compared with that in the normal osteoblast cell line (Fig. 3I). Taken together, these results provide evidence to support a correlation between the expression levels of ZFPM2-AS1 and KIAA1429, and demonstrate that

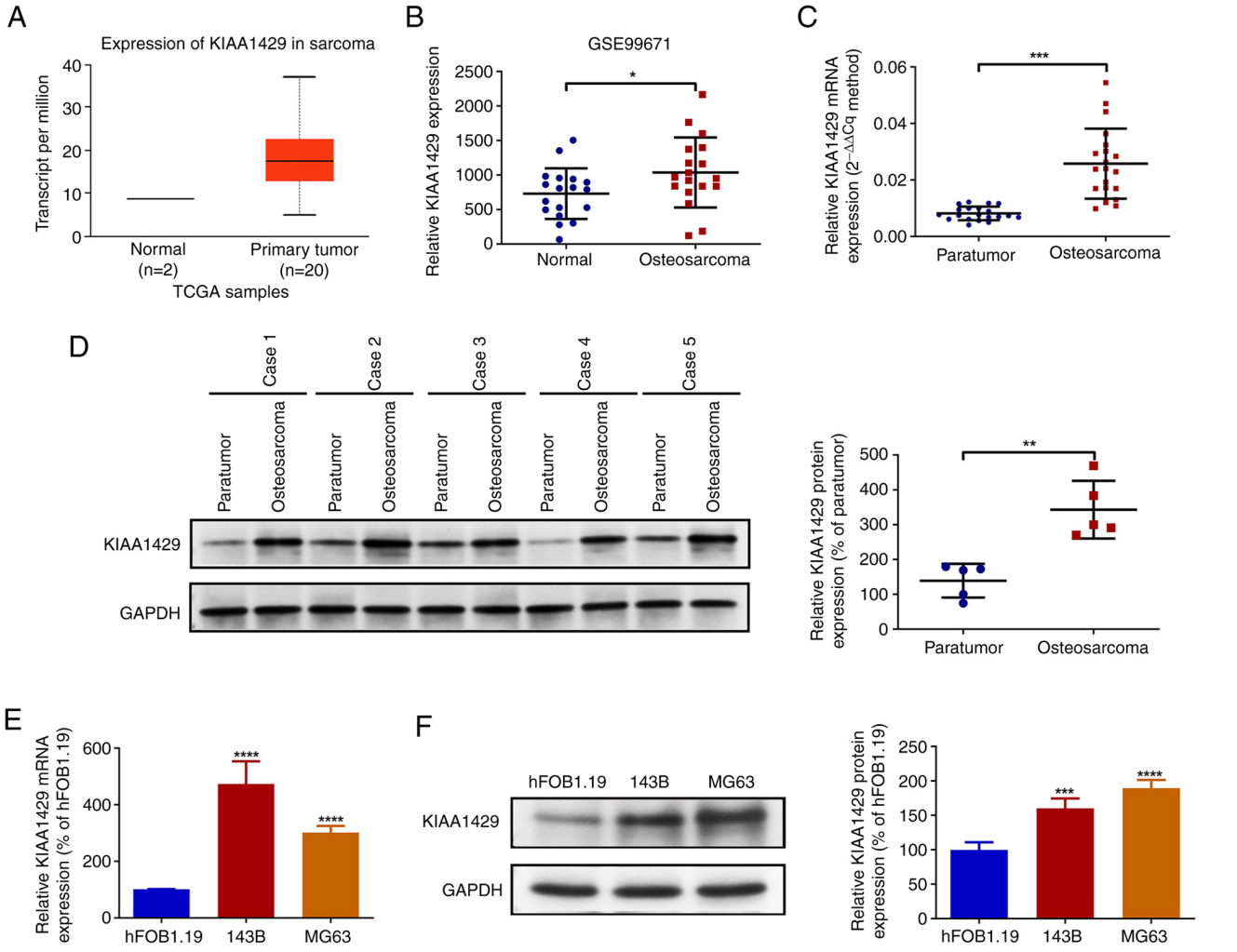

Figure 1. KIAA1429 is upregulated in osteosarcoma tissues and cell lines. (A) KIAA1429 expression in the sarcoma dataset from TCGA database, analyzed using UALCAN. P<0.05 primary tumor vs. normal. (B) KIAA1429 expression in 18 pairs of osteosarcoma tissues and normal tissues from the GSE99671 dataset. *P<0.05 as indicated. (C) Expression of KIAA1429 mRNA in 20 pairs of osteosarcoma tissues and paraneoplastic tissues detected by RT-qPCR analysis. ***P<0.001 as indicated. (D) KIAA1429 protein expression in 5 pairs of osteosarcoma tissues and paraneoplastic tissues detected by western blotting. **P<0.01 as indicated. Expression of KIAA1429 in hFOB1.19, 143B and MG63 cells detected by (E) RT-qPCR analysis and (F) western blotting. ***P<0.001 and ****P<0.0001 vs. hFOB1.19. The data from the *in vitro* experiments are presented as the mean ± SD from three independent experiments. TCGA, The Cancer Genome Atlas; RT-qPCR, reverse transcription-quantitative PCR.

the expression of ZFPM2-AS1 is upregulated in osteosarcoma tissues and cells.

SRAMP predicted m^{6}A modification sites at positions 579, 613, 624, 750, 780 and 833 of the ZFPM2-AS1 sequence, spanning ~260 base pairs. (Fig. S1A). Primers were designed based on the gene regions containing these predicted modification sites, and the m^{6}A methylation level of ZMIZ1-AS1 in osteosarcoma tissues and cells was determined by MeRIP-qPCR. The results revealed that the m^{6}A methylation level of ZFPM2-AS1 was significantly elevated in osteosarcoma tissues and cells in comparison with the levels observed in paraneoplastic tissues and hFOB1.19 cells, respectively (Fig. 3J and K). To further investigate the regulatory role of KIAA1429, the m^{6}A methylation levels of ZFPM2-AS1 were examined via MeRIP-qPCR assay in 143B and MG63 cells following KIAA1429 knockdown. The knockdown of KIAA1429 was observed to result in a significant reduction in the m^{6}A methylation level of ZFPM2-AS1 compared with that in the shNC group (Fig. 3L and M). In addition, an actinomycin D assay revealed that the knockdown of KIAA1429 shortened the half-life of ZFPM2-AS1, indicating that its stability was reduced (Fig. 3N and O). Considered together, these findings suggest that m^{6}A methylation levels of ZFPM2-AS1 are elevated in osteosarcoma tissues and cells. Furthermore, based on the observed reduction following KIAA1429 knockdown, the results suggest that KIAA1429 may increase the m^{6}A methylation levels of ZFPM2-AS1 and promote its stability.

ZFPM2-AS1 knockdown attenuates the promotive effect of KIAA1429 on the proliferation, migration and invasion of osteosarcoma cells. Finally, the impact of ZFPM2-AS1 on KIAA1429-mediated osteosarcoma proliferation, migration and invasion was investigated. First, a cell model with stable overexpression of KIAA1429 was established in 143B and MG63 cells, and the successful construction of the model was verified via western blotting (Fig. 4A and B). Subsequently, siZFPM2-AS1 was transfected into 143B and MG63 cells, resulting in significantly reduced ZFPM2-AS1 expression

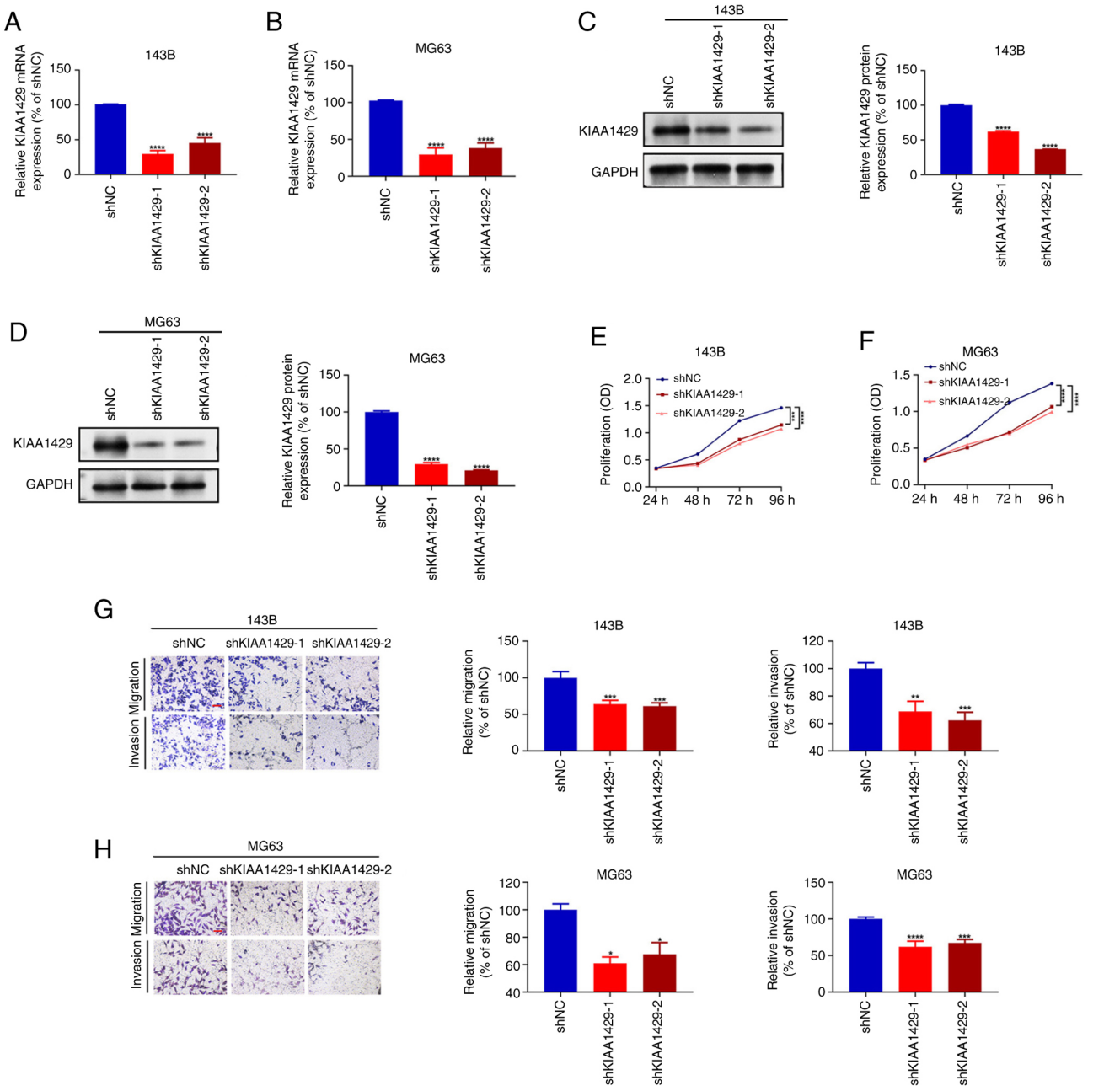

Figure 2. KIAA1429 knockdown inhibits the proliferation, migration and invasion of osteosarcoma cells. Expression levels of KIAA1429 mRNA in (A) 143B and (B) MG63 cells detected by reverse transcription-quantitative PCR and KIAA1429 protein in (C) 143B and (D) MG63 cells detected by western blotting following KIAA1429 knockdown. Proliferation of transfected (E) 143B and (F) MG63 cells detected by Cell Counting Kit-8 assay. Migration and invasion of transfected (G) 143B and (H) MG63 cells detected by Transwell assays (scale bar, 200 μm). All data are presented as the mean ± SD from three independent experiments. *P<0.05, **P<0.01, ***P<0.001 and ****P<0.0001 vs. shNC. shKIAA1429, shRNA targeting KIAA1429; shNC, negative control shRNA; shRNA, short hairpin RNA; OD, optical density.

levels compared with those in the respective siNC-transfected cells, as validated by RT-qPCR (Fig. S1D and E). Then, siZFPM2-AS1 was transfected into 143B and MG63 cells overexpressing KIAA1429, and ZFPM2-AS1 expression was quantified by RT-qPCR. The expression level of ZFPM2-AS1 was observed to increase following the overexpression of KIAA1429 compared with that in the empty vector control group, which was consistent with the observed reduction in ZFPM2-AS1 expression following KIAA1429 knockdown (Fig. 4C and D). However, this oeKIAA1429-induced increase in ZFPM2-AS1 expression was attenuated by co-transfection with siZFPM2-AS1 (Fig. 4C and D). Subsequently, CCK-8 and Transwell functional assays were performed. The overexpression of KIAA1429 significantly promoted cell proliferation, migration and invasion compared with that of the vector control cells. However, these effects of KIAA1429 were attenuated following the knockdown of ZFPM2-AS1 in KIAA1429 overexpressing cells (Fig. 4E and H). These findings suggest that the knockdown of ZFPM2-AS1 attenuates the effects of KIAA1429 on the proliferation, migration and invasion of 143B and MG63 cells.

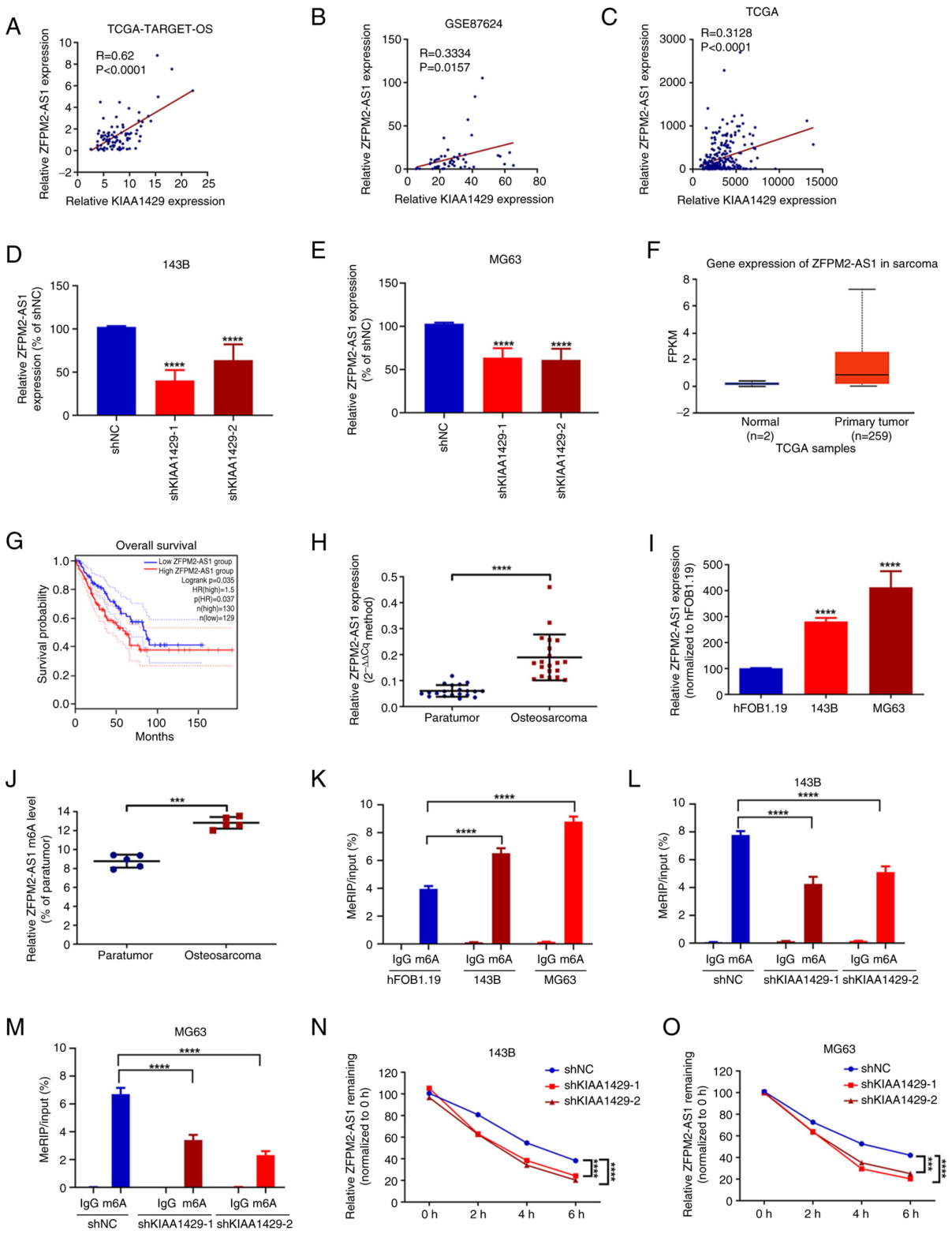

Figure 3. KIAA1429-mediated m^{6}A modification is associated with ZFPM2-AS1 stability in osteosarcoma cells. Correlation of KIAA1429 and ZFPM2-AS1 expression in (A) 87 osteosarcoma tissues from TCGA-TARGET-OS database, (B) 52 osteosarcoma tissues from the GSE87624 osteosarcoma-associated dataset and (C) 260 sarcoma tissues from TCGA. RT-qPCR detection of ZFPM2-AS1 expression in (D) 143B and (E) MG63 cells with KIAA1429 knockdown. ****P<0.0001 vs. shNC. (F) ZFPM2-AS1 expression in sarcoma tissues and normal tissues from TCGA database, analyzed using UALCAN. P<0.001 primary tumor vs. normal. (G) Kaplan-Meier analysis of the overall survival of patients with sarcoma based on ZFPM2-AS1 expression levels. (H) ZFPM2-AS1 expression in 20 pairs of osteosarcoma and paraneoplastic tissues analyzed by RT-qPCR. ****P<0.0001 as indicated. (I) Expression of ZFPM2-AS1 in hFOB1.19, 143B and MG63 cells detected by RT-qPCR. ****P<0.0001 vs. hFOB1.19. m^{6}A levels of ZFPM2-AS1 in (J) 5 pairs of osteosarcoma and paraneoplastic tissues, (K) hFOB1.19, 143B and MG63 cells, and KIAA1429 knockdown (L) 143B and (M) MG63 cells determined by MeRIP-qPCR assay. ***P<0.001 and ****P<0.0001 as indicated. Expression levels of ZFPM2-AS1 determined by RT-qPCR assay in KIAA1429 knockdown (N) 143B and (O) MG63 cells at various time points after the addition of actinomycin D. ***P<0.001 and ****P<0.0001 as indicated. All data are presented as the mean ± SD from three independent experiments. m^{6}A, N^6-methyladenosine; ZFPM2-AS1, friend of GATA family member 2-antisense 1; TCGA, The Cancer Genome Atlas; OS, osteosarcoma; RT-qPCR, reverse transcription-quantitative PCR; shNC, negative control shRNA; shKIAA1429, shRNA targeting KIAA1429; shRNA, short hairpin RNA; FPKM, fragments per kilobase of transcript per million mapped reads; MeRIP, m^{6}A-methylated RNA immunoprecipitation.

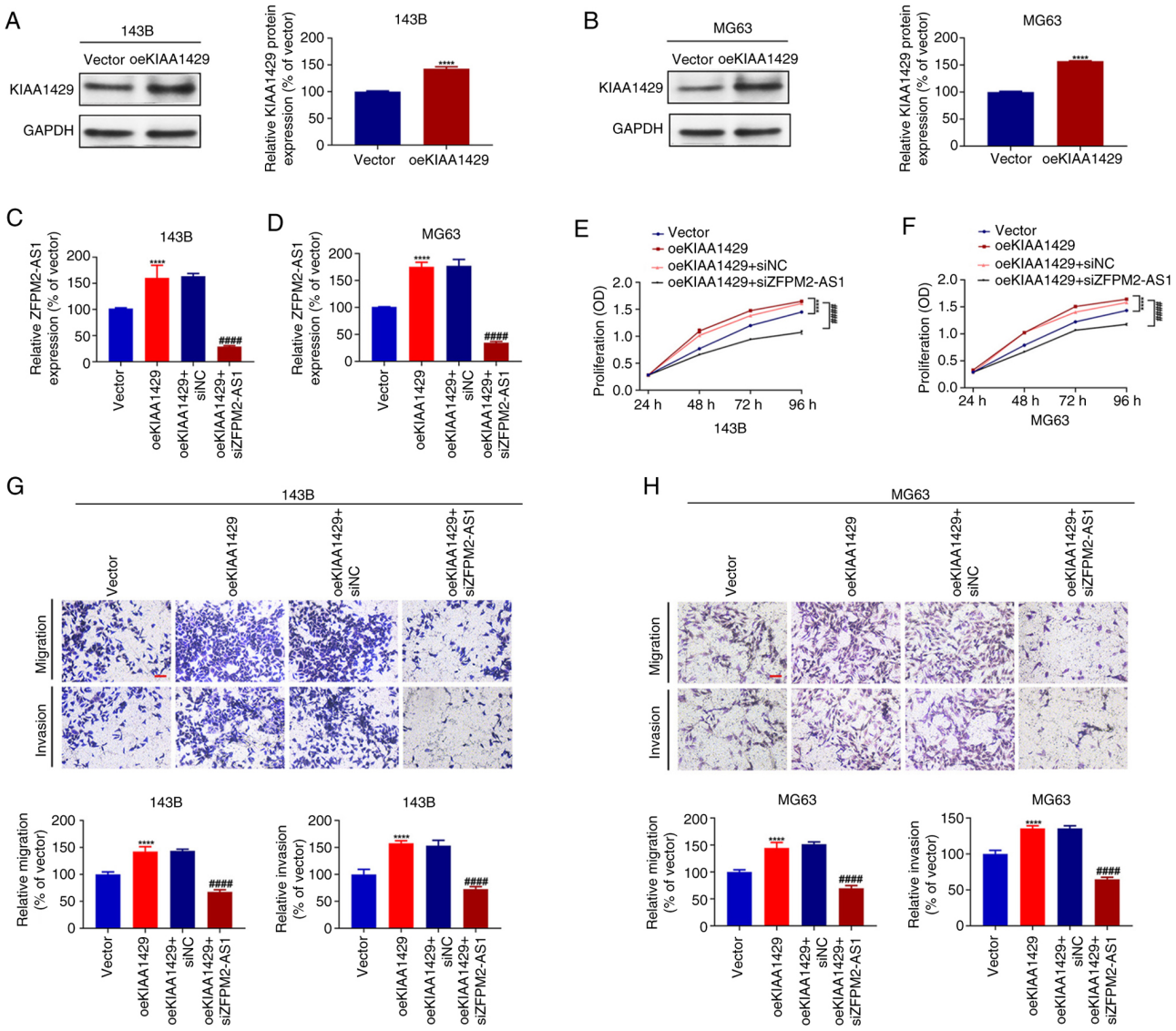

Figure 4. ZFPM2-AS1 knockdown partially attenuates the stimulatory effect of KIAA1429 on the proliferation, migration and invasion of osteosarcoma cells. Western blot analysis of KIAA1429 protein expression in (A) 143B and (B) MG63 cells transfected with oeKIAA1429. ****P<0.0001 vs. vector. Expression of ZFPM2-AS1 in (C) 143B and (D) MG63 cells transfected with oeKIAA1429 alone or in combination with siZFPM2-AS1 as detected by reverse transcription-quantitative PCR analysis. Proliferation of the transfected (E) 143B and (F) MG63 cells detected by Cell Counting kit-8 assay, and the migration and invasion of the (G) 143B and (H) MG63 cells evaluated using Transwell assays; scale bar, 200 μm. All data are presented as the mean ± SD from three independent experiments. ****P<0.0001 vs. vector, $^{\#\#\#\#}$P<0.0001 vs. oeKIAA1429 + siNC. ZFPM2-AS1, friend of GATA family member 2-antisense 1; oeKIAA1429, KIAA1429 overexpression; siZFPM2-AS1, siRNA targeting ZFPM2-AS1; siNC, negative control siRNA; siRNA, small interfering RNA.

Discussion

m^{6}A modification is a dynamic and reversible process regulated by m^{6}A methylation-associated enzymes, which are classified into three categories: Writers, erasers and readers. The methylation reaction is catalyzed by a methyltransferase complex composed of m^{6}A writers such as METTL3, along with METTL14, WTAP and KIAA1429, which performs a key role in the m^{6}A methylation process. By contrast, two demethylating enzymes, namely AlkB homolog 5, which is an RNA-specific demethylase, and fat mass and obesity-associated protein, function as erasers, reversing the methylation of m^{6}A. Furthermore, m^{6}A-binding proteins, including YTHDF1, YTHDF2, YTHDF3 and YTHDC1, act as readers that regulate downstream processes including the translation and degradation of m^{6}A-modified RNAs. The m^{6}A methyltransferases, METTL3, METTL14 and WTAP, have been extensively studied in various types of tumors, including osteosarcoma. KIAA1429 serves as a scaffold within the m^{6}A methyltransferase complex and is its largest known component. It helps coordinate the positioning of the core METTL3/METTL14/WTAP component on RNA substrates for site-specific m^{6}A methylation, particularly near to the 3'-untranslated region and stop codon. In the present study, analysis of data from the GEO and TCGA databases, combined with mRNA and protein profiling, revealed that KIAA1429 expression is upregulated in osteosarcoma tissues and cells. In addition, the knockdown of KIAA1429 inhibited the proliferation, migration and invasion of osteosarcoma cells. Previous studies have demonstrated that KIAA1429 can mediate the m^{6}A modification of lncRNAs, including LINC00667 (27), LINC00958 (28), POU6F2-AS1 (29) and LINC01106 (20),

contributing to tumorigenesis. The present study focused on the role of KIAA1429 in the modification of ZFPM2-AS1 in osteosarcoma.

ZFPM2-AS1 was first reported to play a role in gastric cancer in 2018 (30), and has since been implicated in colorectal cancer (31), esophageal squamous cell carcinoma (22), lung adenocarcinoma (32) and several other tumor types (33). However, to the best of our knowledge, its specific role in osteosarcoma has not previously been reported. In the present study, a positive correlation between KIAA1429 and ZFPM2-AS1 expression was identified in osteosarcoma via bioinformatic and RT-qPCR analyses. ZFPM2-AS1 expression was found to be upregulated in osteosarcoma and the high expression of ZFPM2-AS1 was significantly associated with a poor prognosis in patients with sarcoma. Regarding the underlying mechanism by which ZFPM2-AS1 exerts its pro-cancer effects, previous studies have focused on its function as a competitive endogenous RNA. The m^6A modification of KIAA1429 has been shown to affect the stability of lncRNAs, including LINC00958 (28). In the present study, six possible m^6A modification sites were identified in the ZFPM2-AS1 gene sequence, and KIAA1429 was found to increase both the m^6A level and stability of ZFPM2-AS1. Furthermore, ZFPM2-AS1 knockdown partially attenuated the pro-proliferative, migratory and invasive effects of KIAA1429 on osteosarcoma cells.

The influence of m^6A modification on RNA stability is complex and involves numerous factors. m^6A modification can either enhance or reduce the recognition of RNA by m^6A-reading proteins, such as YTHDFs, YTHDC1 and insulin-like growth factor 2 mRNA-binding proteins. The resulting changes in RNA can lead to either stabilization or degradation through distinct regulatory mechanisms (34). For example, a previous study revealed that m^6A-containing RNAs with heat-responsive protein 12 (HRSP12)-binding sites near to RNase P/MRP-directed cleavage sites are preferentially targeted for endoribonucleolytic cleavage through the YTHDF2-HRSP12-RNase P/MRP axis (35). In addition, in acute myeloid leukemia, the binding of YTHDC1 to nuclear m^6A transcripts promotes the formation of nuclear condensates, thereby safeguarding nuclear mRNAs, such as Myc, from poly (A) tail exosome targeting complex-mediated degradation (36). The actinomycin D experiments performed in the present study demonstrated that the knockdown of KIAA1429 shortened the half-life of the KIAA1429-modified lncRNA ZFPM2-AS1, indicating that its stability was reduced. However, further research is necessary to ascertain the precise underlying mechanism of action.

In summary, in the present study, the expression levels of KIAA1429 and ZFPM2-AS1 in osteosarcoma tissues and cells were analyzed, and their roles in promoting the proliferation, migration and invasion of osteosarcoma cells were revealed. The findings suggest that KIAA1429 contributes to the stability of ZFPM2-AS1 through m^6A modification. However, more in-depth studies are required to identify the specific m^6A modification sites that mediate the interaction between KIAA1429 and ZFPM2-AS1, and to determine whether other m^6A-associated enzymes are involved in the regulation of ZFPM2-AS1. Despite these remaining issues, the present study has identified a potential novel therapeutic target for the molecular therapy of osteosarcoma.

Acknowledgements

Not applicable.

Funding

No funding was received.

Availability of data and materials

The data generated in the present study may be requested from the corresponding author.

Authors' contributions

XB and YZ participated in experimental design discussions. XB conceived and designed the study, supervised the project and acquired funding. XB and YB performed the key experiments. YB and YZ were responsible for data acquisition and processing (YB validated data and YZ processed the preliminary data while verifying raw data authenticity). HZ, CL, and HS performed the statistical analysis, interpreted experimental data and validated results. KG performed independent data analysis and biological interpretation of key findings. YZ conducted the literature analysis and prepared all figures and visualization materials. YZ drafted the initial manuscript. KG and XB critically revised the manuscript (KG optimized experimental protocols, established data quality control criteria, validated data integrity and reproducibility, and revised for methodological accuracy and biological interpretation while XB revised the manuscript for intellectual content). KG and XB confirm the authenticity of all the raw data. All authors have read and approved the final version of the manuscript.

Ethics approval and consent to participate

The Medical Ethics Committee of Central Hospital Affiliated to Shenyang Medical College approved the use of clinical tissue specimens from Central Hospital Affiliated to Shenyang Medical College and Liaoning Provincial Cancer Hospital in this study (approval no, 2022DEC12-7). All adult participants and the parents or legal guardians of participants <18 years of age provided written informed consent for participation.

Patient consent for publication

Not applicable.

Competing interests

The authors declare that they have no competing interests.

References

1. Bielack SS, Kempf-Bielack B, Delling G, Exner GU, Flege S, Helmke K, Kotz R, Salzer-Kuntschik M, Werner M, Winkelmann W, *et al*: Prognostic factors in high-grade osteosarcoma of the extremities or trunk: An analysis of 1,702 patients treated on neoadjuvant cooperative osteosarcoma study group protocols. J Clin Oncol 20: 776-790, 2002.

2. Kansara M, Teng MW, Smyth MJ and Thomas DM: Translational biology of osteosarcoma. Nat Rev Cancer 14: 722-735, 2014.
3. Isakoff MS, Bielack SS, Meltzer P and Gorlick R: Osteosarcoma: Current treatment and a collaborative pathway to success. J Clin Oncol 33: 3029-3035, 2015.
4. Cai Y, Feng R, Lu T, Chen X, Zhou X and Wang X: Novel insights into the m(6)A-RNA methyltransferase METTL3 in cancer. Biomark Res 9: 27, 2021.
5. Chen D, Gu X, Nurzat Y, Xu L, Li X, Wu L, Jiao H, Gao P, Zhu X, Yan D, *et al*: Writers, readers, and erasers RNA modifications and drug resistance in cancer. Mol Cancer 23: 178, 2024.
6. Wang J, Xiu M, Wang J, Gao Y and Li Y: METTL16-SENP3-LTF axis confers ferroptosis resistance and facilitates tumorigenesis in hepatocellular carcinoma. J Hematol Oncol 17: 78, 2024.
7. Yu Y, Yang YL, Chen XY, Chen ZY, Zhu JS and Zhang J: Helicobacter pylori-enhanced hnRNPA2B1 coordinates with PABPC1 to promote Non-m(6)A translation and gastric cancer progression. Adv Sci (Weinh) 11: e2309712, 2024.
8. Mao L, Wang L, Lyu Y, Zhuang Q, Li Z, Zhang J, Gu Z, Lu S, Wang X, Guan Y, *et al*: Branch chain amino acid metabolism promotes brain metastasis of NSCLC through EMT occurrence by regulating ALKBH5 activity. Int J Biol Sci 20: 3285-3301, 2024.
9. Guo X, Qiu W, Li B, Qi Y, Wang S, Zhao R, Cheng B, Han X, Du H, Pan Z, *et al*: Hypoxia-induced neuronal activity in glioma patients polarizes microglia by potentiating RNA m6A demethylation. Clin Cancer Res 30: 1160-1174, 2024.
10. Wei X, Feng J, Chen L, Zhang C, Liu Y, Zhang Y, Xu Y, Zhang J, Wang J, Yang H, *et al*: METTL3-mediated m6A modification of LINC00520 confers glycolysis and chemoresistance in osteosarcoma via suppressing ubiquitination of ENO1. Cancer Lett: August 29, 2024 (Ebup ahead of print).
11. Knuckles P, Lence T, Haussmann IU, Jacob D, Kreim N, Carl SH, Masiello I, Hares T, Villaseñor R, Hess D, *et al*: Zc3h13/Flacc is required for adenosine methylation by bridging the mRNA-binding factor Rbm15/Spenito to the m(6)A machinery component Wtap/Fl(2)d. Genes Dev 32: 415-429, 2018.
12. Zhu W, Wang JZ, Wei JF and Lu C: Role of m6A methyltransferase component VIRMA in multiple human cancers (Review). Cancer Cell Int 21: 172, 2021.
13. Chen X, Lu T, Cai Y, Han Y, Ding M, Chu Y, Zhou X and Wang X: KIAA1429-mediated m6A modification of CHST11 promotes progression of diffuse large B-cell lymphoma by regulating Hippo-YAP pathway. Cell Mol Biol Lett 28: 32, 2023.
14. Luo J, Wang X, Chen Z, Zhou H and Xiao Y: The role and mechanism of JAK2/STAT3 signaling pathway regulated by m6A methyltransferase KIAA1429 in osteosarcoma. J Bone Oncol 39: 100471, 2023.
15. Goodall GJ and Wickramasinghe VO: RNA in cancer. Nat Rev Cancer 21: 22-36, 2021.
16. Fang Y and Fullwood MJ: Roles, functions, and mechanisms of long Non-coding RNAs in cancer. Genomics Proteomics Bioinformatics 14: 42-54, 2016.
17. Luongo M, Laurenziello P, Cesta G, Bochicchio AM, Omer LC, Falco G, Milone MR, Cibarelli F, Russi S and Laurino S: The molecular conversations of sarcomas: exosomal non-coding RNAs in tumor's biology and their translational prospects. Mol Cancer 23: 172, 2024.
18. Shaath H, Vishnubalaji R, Elango R, Kardousha A, Islam Z, Qureshi R, Alam T, Kolatkar PR and Alajez NM: Long non-coding RNA and RNA-binding protein interactions in cancer: Experimental and machine learning approaches. Semin Cancer Biol 86(Pt 3): 325-345, 2022.
19. Shi Q, Chu Q, Zeng Y, Yuan X, Wang J, Zhang Y, Xue C and Li L: Non-coding RNA methylation modifications in hepatocellular carcinoma: Interactions and potential implications. Cell Commun Signal 21: 359, 2023.
20. Xu D, Wang Z and Li F: KIAA1429 Induces m6A Modification of LINC01106 to enhance the malignancy of lung adenocarcinoma cells via the JAK/STAT3 pathway. Crit Rev Immunol 44: 49-61, 2024.
21. Han S, Cao D, Sha J, Zhu X and Chen D: LncRNA ZFPM2-AS1 promotes lung adenocarcinoma progression by interacting with UPF1 to destabilize ZFPM2. Mol Oncol 14: 1074-1088, 2020.
22. Sun G and Wu C: ZFPM2-AS1 facilitates cell growth in esophageal squamous cell carcinoma via up-regulating TRAF4. Biosci Rep 40: BSR20194352, 2020.
23. Ren R, Du Y, Niu X and Zang R: ZFPM2-AS1 transcriptionally mediated by STAT1 regulates thyroid cancer cell growth, migration and invasion via miR-515-5p/TUSC3. J Cancer 12: 3393-3406, 2021.
24. Chandrashekar DS, Bashel B, Balasubramanya SAH, Creighton CJ, Ponce-Rodriguez I, Chakravarthi BVSK and Varambally S: UALCAN: A portal for facilitating tumor subgroup gene expression and survival analyses. Neoplasia 19: 649-658, 2017.
25. Tang Z, Kang B, Li C, Chen T and Zhang Z: GEPIA2: An enhanced web server for large-scale expression profiling and interactive analysis. Nucleic Acids Res 47(W1): W556-W560, 2019.
26. Zhou Y, Zeng P, Li YH, Zhang Z and Cui Q: SRAMP: Prediction of mammalian N6-methyladenosine (m6A) sites based on sequence-derived features. Nucleic Acids Res 44: e91, 2016.
27. Ren S, Zhang Y, Yang X, Li X, Zheng Y, Liu Y and Zhang X: N6-methyladenine-induced LINC00667 promoted breast cancer progression through m6A/KIAA1429 positive feedback loop. Bioengineered 13: 13462-13473, 2022.
28. Yang D, Chang S, Li F, Ma M, Yang J, Lv X, Huangfu L and Jia C: m(6) A transferase KIAA1429-stabilized LINC00958 accelerates gastric cancer aerobic glycolysis through targeting GLUT1. IUBMB Life 73: 1325-1333, 2021.
29. Lu D and Chen A: lncRNA POU6F2-AS1 regulated by KIAA1429 contributes to colorectal cancer progression in an m(6)A modification manner. Mol Biotechnol 67: 115-122, 2025.
30. Kong F, Deng X, Kong X, Du Y, Li L, Zhu H, Wang Y, Xie D, Guha S, Li Z, *et al*: ZFPM2-AS1, a novel lncRNA, attenuates the p53 pathway and promotes gastric carcinogenesis by stabilizing MIF. Oncogene 37: 5982-5996, 2018.
31. Xiao M, Liang Z and Yin Z: Long non-coding RNA ZFPM2-AS1 promotes colorectal cancer progression by sponging miR-137 to regulate TRIM24. Mol Med Rep 23: 98, 2021.
32. Xue M, Tao W, Yu S, Yan Z, Peng Q, Jiang F and Gao X: lncRNA ZFPM2-AS1 promotes proliferation via miR-18b-5p/VMA21 axis in lung adenocarcinoma. J Cell Biochem 121: 313-321, 2020.
33. Tan F: ZFPM2-AS1: An oncogenic long non-coding RNA in multiple cancer types. Mini Rev Med Chem 23: 88-98, 2023.
34. Zhang Y, Xu Y, Bao Y, Luo Y, Qiu G, He M, Lu J, Xu J, Chen B and Wang Y: N6-methyladenosine (m6A) modification in osteosarcoma: expression, function and interaction with noncoding RNAs-an updated review. Epigenetics 18: 2260213, 2023.
35. Park OH, Ha H, Lee Y, Boo SH, Kwon DH, Song HK and Kim YK: Endoribonucleolytic cleavage of m(6)A-Containing RNAs by RNase P/MRP complex. Mol Cell 74: 494-507.e8, 2019.
36. Cheng Y, Xie W, Pickering BF, Chu KL, Savino AM, Yang X, Luo H, Nguyen DT, Mo S, Barin E, *et al*: N(6)-Methyladenosine on mRNA facilitates a phase-separated nuclear body that suppresses myeloid leukemic differentiation. Cancer Cell 39: 958-972.e8, 2021.